

Comparison of MPC and PI Controller for Grid-Connected Cascade Inverter

M. Pastor¹, J. Dudrik¹

¹Dept. of Electrical Engineering and Mechatronics, Faculty of Electrical Engineering and Informatics, Technical University of Kosice, Letna 9, 042 00 Kosice, Slovakia
marek.pastor@tuke.sk

Abstract—The paper describes and compares the dynamic performance of the PI and the MPC controllers used with the one-phase multilevel cascade inverter connected to the grid through an LCL filter. The cascade inverter uses multilevel sinusoidal PWM modulation technique and is controlled in rotating reference frame. The PI controller uses active damping using virtual resistance to damp oscillations of LCL filter. The MPC controller results present its ability to stabilise unstable plants and no additional active damping technique is necessary to stabilise the LCL filter. Both controllers have the same sampling time.

Index Terms— LCL filter, model predictive control, multilevel inverter.

I. INTRODUCTION

Model predictive control (MPC) has been used for decades in process engineering. With the help of fast microcontrollers, the MPC is being used to control power electronics and electrical drives [1]. Traditionally PID controllers were, and still are, used in this area. Also modern control techniques such as neural networks are used in this area [2]. The MPC offers many advantages such as optimal control technique which requires a rather exact model of the controlled system [3]. These advantages are presented in literature but only few examples compare MPC control technique to the well-established PID control in the area of power electronics and electrical drive control [1], [4], [5].

This paper describes the performance of both, PI and MPC, controllers applied to the same system. The system is a grid connected multilevel cascade inverter with output LCL filter. It is not a fast dynamics requiring system but is unstable without additional damping. The MPC has ability to stabilize unstable processes and to predict the best control move to achieve a fast dynamic response [6]. The PI controller must include an additional damping technique which usually requires an extra sensor [7].

II. SYSTEM MODEL

The simulated system of a grid connected one-phase cascade inverter consists of several basic parts described in this section. The overall scheme is shown in Fig. 1.

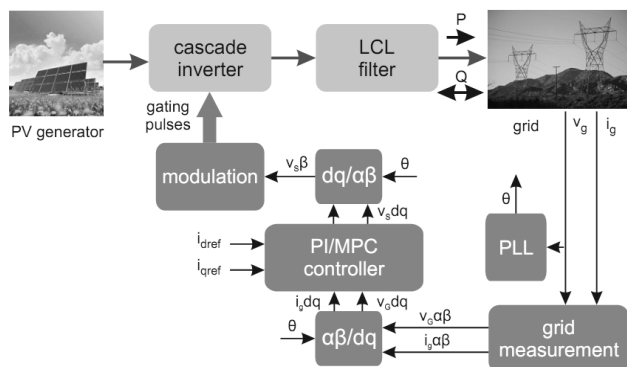


Fig. 1. Grid-connected cascade multilevel inverter with LCL output filter controlled by PI or MPC controller.

A. Multilevel Inverter

The described system includes cascade H-bridge multilevel inverter with three separated dc sources with unequal voltage levels. The inverter is capable of creating 15 levels of output voltage V_s .

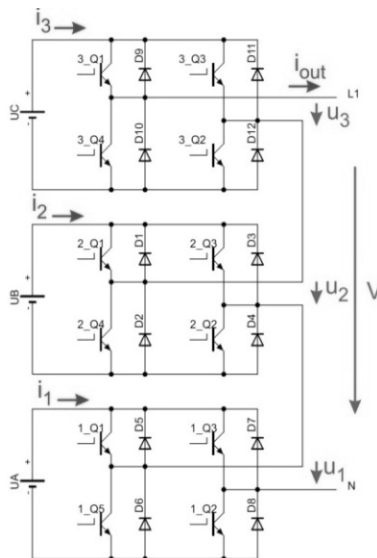


Fig. 2. 15-level cascade H-bridge multilevel inverter.

B. LCL Filter Model

To design the controller, it is necessary to know the system model. The inverter is connected to the grid through an LCL filter to eliminate high-frequency harmonics

Manuscript received December 18, 2013; accepted March 5, 2014.
This work was supported by the Slovak Research and Development Agency under the contract No. APVV-0185-10.

produced by PWM inverter [8]. Both, MPC and PI controllers use a modulator to produce multilevel PWM. The time delay of the inverter is negligible due to the high frequency PWM. In order to design the controller it is necessary to know the model of the LCL filter. The LCL filter uses active damping to remove losses produced by passive damping [7].

The state space model of the LCL filter is derived in rotating reference frame dq due to the use of PI controller (see Appendix A). The PR controller implemented in stationary reference frame could be used as well. The input matrix B_{sdq} includes the disturbance represented by grid voltage V_G . To check the controllability of the system it is necessary to split the input matrix B_{sdq} between control input V_S and measured disturbance V_G . However inputs and measured disturbances combined into one input matrix are not a problem for MPC. There is possibility to specify the type of the system inputs during an MPC controller design.

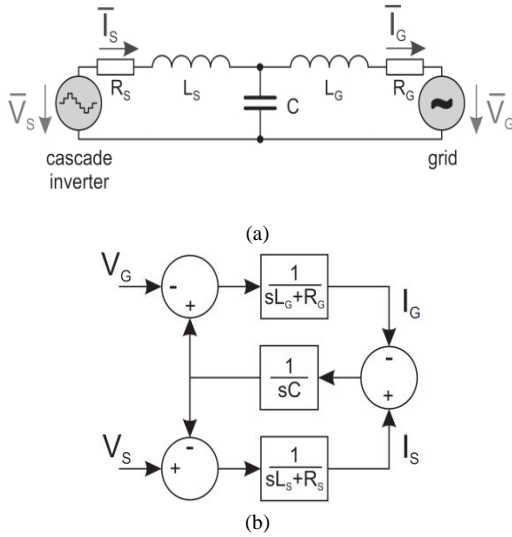


Fig. 3. LCL filter topology and dynamic model.

TABLE I. PARAMETERS OF THE LCL FILTER AND INVERTER.

Parameter	Symbol	Value
Apparent power	S	4.6 kW
Switching frequency	f_{sw}	10 kHz
Inverter side inductor	L_S	0.27 mH
Grid side inductor	L_G	0.13 mH
Capacitor	C	18 μ F
Resistance of L_G	R_G	10 m
Resistance of L_S	R_S	10 m
First H-bridge DC link	U_A	240 V
Second H-bridge DC link	U_B	120 V
Third H-bridge DC link	U_C	60 V

C. Modulation Technique

Both controllers, MPC as well as PI, use modulator and have thus a fixed switching frequency. The MPC controller is implemented with Continuous Control Set. It helps to compare both controllers and prevents possible problems which could arise from using Finite Control Set MPC with variable switching frequency. The multilevel modulator uses 14-level shifted carrier signals (Fig. 4).

The amplitude modulation index m_a of the multilevel inverter is defined (A_m – amplitude of modulation signal, A_c – amplitude of carrier signal, m – number of levels of output voltage)

$$m_a = \frac{A_m}{(m-1)A_c}. \quad (1)$$

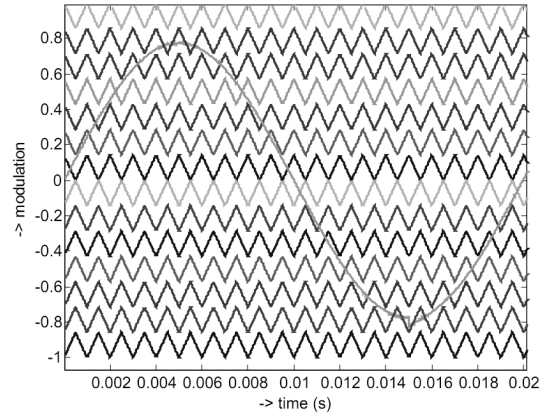


Fig. 4. Multilevel modulation technique used in the inverter ($m_r = 20$).

The frequency modulation index m_f of the multilevel inverter is defined (f_c – frequency of carrier signal, f_g – grid frequency)

$$m_f = \frac{f_c}{f_g}. \quad (2)$$

III. PI CONTROLLER

To design the PI controller it is necessary to know the transfer function from inverter voltage V_S (manipulated variable) to grid current I_G (controlled variable). The grid voltage is a measured disturbance and is compensated in the PI controller. The high frequency transfer function from V_S to I_G is

$$\frac{I_G}{V_S} = \frac{1}{s^3 L_S L_G C + s^2 (L_S C R_G + R_S C L_G) + s (R_S C R_G + L_S + L_G) + R_S + R_G}. \quad (3)$$

The PI controller controls the grid current I_G with grid frequency and thus generates the manipulated variable V_S with grid frequency. The transfer function (3) is simplified by omitting the high-frequency terms

$$\frac{I_G}{V_S} \Big|_{LL} = \frac{1}{s(L_S + L_G) + R_S + R_G}. \quad (4)$$

The LCL filter is therefore simplified to first order system with time constant of

$$T_{LCL} = \frac{L_S + L_G}{R_S + R_G}, \quad (5)$$

and gain of

$$K_{LCL} = \frac{1}{R_S + R_G}. \quad (6)$$

The PI controller is designed to compensate the time constant T_{LCL} . The proportional gain of the PI controller is set to (τ is time constant of required control dynamics)

$$K_P = \frac{T_{LCL}}{\dagger K_{LCL}}. \quad (7)$$

The integral gain of PI controller is set to

$$K_I = \frac{K_P}{T_{LCL}}. \quad (8)$$

The PI controller is implemented in discrete form with sampling time T and manipulated variable $u(kT)$ defined as

$$u(kT) = u(kT-1) + K_1 e(kT) + K_2 e(kT-1), \quad (9)$$

where:

$$\begin{cases} K_1 = K_P + K_I T/2, \\ K_2 = -K_P + K_I T/2. \end{cases} \quad (10)$$

The LCL filter has three reactive elements and thus can resonate if supplied by signals with energies on resonant frequencies. Thus the LCL filter needs to be damped in order to prevent oscillations.

There are two possibilities how to prevent resonances – active and passive damping.

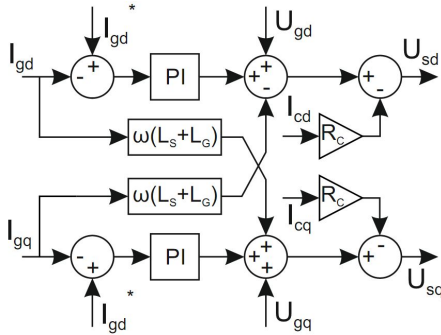


Fig. 5. Structure of PI controller with active damping in rotating reference frame.

The active damping is preferable with regards to the efficiency of the system. The active damping of an LCL filter can be realised by using virtual resistor method, by using capacitor current controller or by incorporating the notch filter [7]. The virtual resistor method was selected for this paper. This method requires measurement of the capacitor current but can be considered more robust than the notch filter. The structure of the PI controller in rotating reference frame with virtual resistor R_c is shown in Fig. 5.

TABLE II. PARAMETERS OF THE PI CONTROLLER.

Parameter	Symbol	Value
Proportional gain	K_P	0.8
Integral gain	K_I	40
Required dynamics		0.5 ms
Discrete gain	K_1	0.8002
Discrete gain	K_2	0.7998
Sampling time	T	10 μ s
Virtual resistor	R_c	0.74

IV. MODEL PREDICTIVE CONTROL

Model Predictive Control (MPC) is an advanced digital

control technique used in process industry from 1980s. The MPC uses a dynamical model of the system. The optimal control move is computed on-line by solving an open-loop optimization problem at each sampling time. The optimal sequence of the manipulated variable is calculated over control horizon based on the current system space. Only the first control move is applied to the system. This is the opposite to the pre-computed control law such as PI control where the closed-loop performance is considered [9].

The advantages of MPC are ease of multivariable control tasks and avoiding of the cascade control structure. Features such as high dynamics, ability to handle unstable processes (the case of LCL filter without damping), consideration of actuators mechanical limitations, and the easy tuning of the MPC controller are considered as well. The main disadvantages are need of exact system model and possible instability when the prediction horizon is not defined correctly.

From power electronics point of view, the MPC is divided into two main categories according to the control set – Finite Control Set (FCS) MPC and Continuous Control Set (CCS) MPC [1]. The first one does not require a modulator and has a variable switching frequency. The second one uses a modulator and thus uses a constant switching frequency. Each one of these approaches has its advantages. The CCS MPC was used for this work as it can be easily compared to the PI controller.

The MPC is a multivariable control algorithm. The calculation of the optimal control move is based on solving the optimization problem defined by a cost function. For MPC the cost function for MIMO system has a general form of [10]

$$J = \min_{\Delta u} \left(\sum_{k=0}^{N_p-1} \left(\sum_{j=1}^{n_y} \|W_{i+1,j}^y (y_j(k+i+1|k) - r_j(k+i+1))\|^2 + \sum_{j=1}^{n_u} \|W_{i,j}^{\Delta u} \Delta u_j(k+i|k)\|^2 \right) \right), \quad (11)$$

subjected to constrains

$$\begin{cases} u_{\min} \leq u(t+k) \leq u_{\max}, k = 0, \dots, N_p - 1, \\ \Delta u_{\min} \leq \Delta u(t+k) \leq \Delta u_{\max}, k = 0, \dots, N_c - 1, \\ y_{\min} \leq u(t+k) \leq y_{\max}, k = 0, \dots, N_p, \\ \Delta u(t+k) = 0, k = N_c, \dots, N_p - 1, \end{cases} \quad (12)$$

where N_p – prediction horizon, N_c – control horizon, W^y – output variables weight, W^u – manipulated variable rate weight, n_y – number of outputs, n_u – number of inputs, y – system output, r – output set-point, u – manipulated variable rate.

The multilevel inverter is controlled in rotating reference frame. The MPC controller has 3 inputs (grid current in dq, grid voltage in dq, reference set-points in dq) and one output (required inverter voltage in dq). The state variables are observed by the Kalman filter [10].

To tune the MPC controller it is only possible to change the prediction and control horizons, the output and manipulated variable weights and then to simulate the response of the designed controller. The MPC controller output rate of change depends on these parameters. In general, the controller with large u can be a problem, eq. when some actuators are used. But in power electronics such problem does not occur. However, increasing prediction and control horizons result in smaller u .

TABLE III. PARAMETERS OF THE MPC CONTROLLER.

Parameter	Symbol	Value
Output variables weight	W^y	1.4918
Manipulated variables rate weight	W^u	0.067
Prediction horizon	N_p	10
Control horizon	N_c	2
Sampling time	T	$10 \mu\text{s}$

V. SIMULATION

To verify the PI and MPC controller design, both discrete controllers were simulated in Matlab/Simulink. The cascade inverter supplied power to one phase grid 230 V/50 Hz. Initial required grid current was set to 0 A and then at 0.015 s was stepped to $I_{g\max} = 25$ A. Power factor was set to 1 and power supplied to the grid was 4 kW. Simulation results are presented in Fig. 6 and Fig. 7.

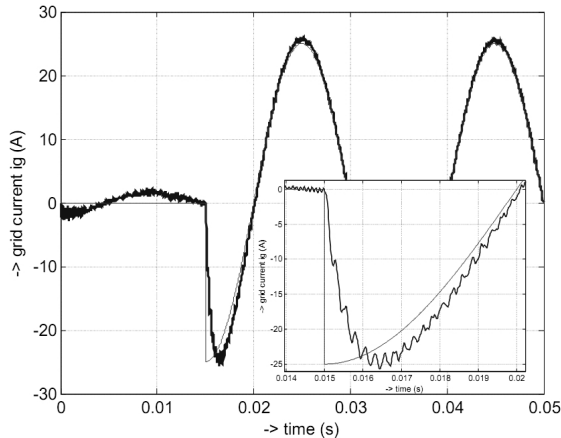


Fig. 6. Grid current control by PI controller. The reference grid current I_d was stepped in 0.015 s from 0 A to 25 A. I_q current was held at 0.

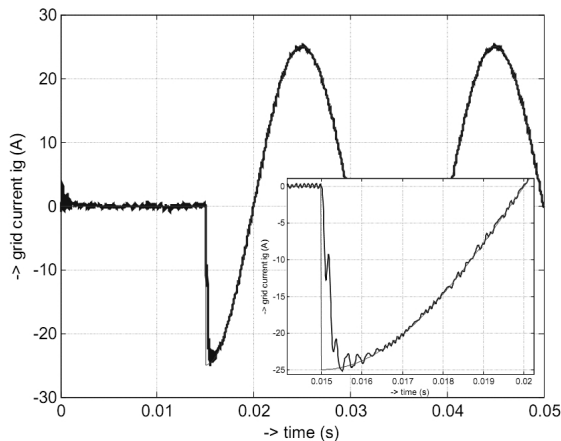


Fig. 7. Grid current control by MPC controller. The reference grid current I_d was stepped in 0.015 s from 0 to 25 A. I_q current was held at 0.

It can be seen that the PI controller would take longer time to cancel the grid current to zero. And its response was

also a bit slower after the step change in required grid current I_{Gd} . The MPC controller has no problem with quick cancelling of the grid current and its response to step change in I_{Gd} was also faster. The dynamics of the PI controller could be set faster. However, the system becomes unstable for larger gain of the PI controller. From simulation results it can be seen that the MPC controller can naturally stabilise the unstable LCL filter without implementation of any active damping method. The THD of the grid current is for both controllers around 1.2 %.

VI. CONCLUSIONS

The paper presents two widely used control techniques, PI control and MPC control, to control the one-phase multilevel inverter connected to the grid through the LCL filter. Both controllers have the same reference frame transformations, switching frequency and the same modulation technique. From simulation results the MPC controller performance is better. But the difference is not so significant and the PI controller has sufficient dynamics for grid-connected inverter. The advantage of the MPC controller is natural damping of the unstable LCL filter with no additional costs of the extra current sensor compared to the PI controller. The simulation results will be verified on real laboratory model of the inverter.

APPENDIX A

The state space description of the LCL filter in dq frame:

$$\begin{bmatrix} sI_{Gd} \\ sI_{Gq} \\ sI_{Sd} \\ sI_{Sq} \\ sU_{Cd} \\ sU_{Cq} \end{bmatrix} = A_{Sdq} \begin{bmatrix} I_{Gd} \\ I_{Gq} \\ I_{Sd} \\ I_{Sq} \\ U_{Cd} \\ U_{Cq} \end{bmatrix} + B_{Sdq} \begin{bmatrix} U_{Gd} \\ U_{Gq} \\ U_{Sd} \\ U_{Sq} \end{bmatrix}, \quad (\text{A.1})$$

$$\bar{y} = \underbrace{\begin{bmatrix} 1 & 1 & 0 & 0 & 0 & 0 \end{bmatrix}}_{C_{Sdq}} \begin{bmatrix} I_{Gd} \\ I_{Gq} \\ I_{Sd} \\ I_{Sq} \\ U_{Cd} \\ U_{Cq} \end{bmatrix} + \underbrace{\begin{bmatrix} 0 & 0 & 0 & 0 \end{bmatrix}}_{D_{Sdq}} \begin{bmatrix} U_{Gd} \\ U_{Gq} \\ U_{Sd} \\ U_{Sq} \end{bmatrix}, \quad (\text{A.2})$$

where matrixes B_{Sdq} and A_{Sdq} are:

$$B_{Sdq} = \begin{bmatrix} -\frac{1}{L_G} & 0 & 0 & 0 \\ 0 & -\frac{1}{L_G} & 0 & 0 \\ 0 & 0 & \frac{1}{L_S} & 0 \\ 0 & 0 & 0 & \frac{1}{L_S} \\ 0 & 0 & 0 & 0 \\ 0 & 0 & 0 & 0 \end{bmatrix}, \quad (\text{A.3})$$

$$A_{Sdq} = \begin{bmatrix} -\frac{R_G}{L_G} & \dot{\xi} & 0 & 0 & \frac{1}{L_G} & 0 \\ -\dot{\xi} & -\frac{R_G}{L_G} & 0 & 0 & 0 & \frac{1}{L_G} \\ 0 & 0 & -\frac{R_S}{L_S} & \dot{\xi} & -\frac{1}{L_S} & 0 \\ 0 & 0 & -\dot{\xi} & -\frac{R_S}{L_S} & 0 & -\frac{1}{L_S} \\ -\frac{1}{C} & 0 & \frac{1}{C} & 0 & 0 & \dot{\xi} \\ 0 & -\frac{1}{C} & 0 & \frac{1}{C} & -\dot{\xi} & 0 \end{bmatrix}. \quad (\text{A.4})$$

REFERENCES

- [1] J. Rodriguez, P. Cortes, *Predictive Control of Power Converters and Electrical Drives*, Wiley-IEEE Press, 2012, p. 230. [Online]. Available: <http://dx.doi.org/10.1002/9781119941446>
- [2] P. Girovsky, J. Zilkova, J. Timko, J. Girovsky, “An adaptive neurocontroller for induction motors”, *Communications*, vol. 15, no. 3, pp. 68–72, 2013.
- [3] L. Wang, *Model Predictive Control System Design and Implementation using Matlab*, Springer, 2009, p. 375.
- [4] A. M. Kassen, A. A. Hassan, “Performance improvements of a permanent magnet synchronous machine via functional model predictive control”, *Journal of Control Science and Engineering*, 2012, p. 8. [Online]. Available: <http://dx.doi.org/10.1155/2012/319708>
- [5] K. Belda, “Study of predictive control for permanent magnet synchronous motor drives”, in *IEEE Proc. Methods and Models in Automation and Robotics (MMAR)*, 2012, pp. 522–527, [Online]. Available: <http://dx.doi.org/10.1109/MMAR.2012.6347831>
- [6] J. B. Rawlings, K. R. Muske, “The stability of constrained receding horizon control”, *IEEE Trans. Automatic Control*, vol. 38, no. 10, pp. 1512–1516, 1993. [Online]. Available: <http://dx.doi.org/10.1109/9.241565>
- [7] W. Zhao, G. Chen, “Comparison of active and passive damping methods for application in high power active power filter with LCL-filter”, in *IEEE Proc. Sustainable Power Generation and Supply, 2009. (SUPERGEN 2009)*, Nanjing, 2009, pp. 1–6. [Online]. Available: <http://dx.doi.org/10.1109/SUPERGEN.2009.5347992>
- [8] H. Huang, R. Hu, G. Yi, “Research on dual-loop controlled grid-connected inverters on the basis of LCL output filters”, *Elektronika ir Elektrotechnika*, vol. 20, no. 1, pp. 8–14, 2014, [Online]. Available: <http://dx.doi.org/10.5755/j01.eee.20.1.5589>
- [9] L. Dai, Y. Xia, M. Fu, M. S. Mahmoud, “Discrete-time model predictive control”, in *Proc. Advances in Discrete Time Systems, Intech*, pp. 77–116, 2012. [Online]. Available: <http://dx.doi.org/10.5772/51122>
- [10] A. Bemporad, M. Morari, N. L. Ricker, “Model predictive control toolbox, user’s guide”, *MathWorks*, 2012, p. 256.